Absolute Thermodynamic Measurements of Alkali Metal Cation Interactions with a Simple Dipeptide and Tripeptide

S. J. Ye and P. B. Armentrout*

Department of Chemistry, University of Utah, Salt Lake City, Utah 84112

Received: November 8, 2007; In Final Form: January 26, 2008

Absolute bond dissociation energies (BDEs) of glycylglycine (GG) and glycylglycylglycine (GGG) to sodium and potassium cations and sequential bond energies of glycine (G) in Na^+G_2 were determined experimentally by threshold collision-induced dissociation (TCID) in a guided ion beam tandem mass spectrometer. Experimental results showed that the binding energies follow the order of $Na^+ > K^+$ and $M^+GGG > M^+GG > M^+G$. Theoretical calculations at the B3LYP/6-311+G(d) level show that all complexes had charge-solvated structures (nonzwitterionic) with either [CO,CO] bidentate or [N,CO,CO] tridentate coordination for M^+GG complexes, [CO,CO,CO] tridentate or [N,CO,CO,CO] tetradentate coordination for M^+GGG complexes, and [N,CO,N,CO] tetradentate coordination for Na^+G_2. Ab initio calculations at three different levels of theory (B3LYP, B3P86, and MP2(full) using the 6-311+G(2d,2p) basis set with geometries and zero-point energies calculated at the B3LYP/6-311+G(d) level) show good agreement with the experimental bond energies. This study demonstrates for the first time that TCID measurements of absolute BDEs can be successfully extended to biological molecules as complex as a tripeptide.

1. Introduction

Alkali metal cations, in particular, Na^+ and K^+, play an important role in many biological systems.[1,2] For example, recent molecular dynamics (MD) simulations of sodium cation permeation across the gramicidin A channel showed that the sodium cation interacts with at least three and at most four backbone carbonyl oxygen atoms and two water molecules, forming a pseudo-trigonal bipyramidal or pseudo-octahedral coordination of Na^+ in the channel.[2] Therefore, thermochemical and structural investigation of the intrinsic properties of the pairwise interactions of alkali metal cations with amino acids and small peptides in the gas phase as simple model systems could provide quantitative insight into the biological function of the alkali metal cation in vivo.

Gas-phase studies of alkali metal cations binding to isolated amino acids have been abundant for several years. For example, it is known that the alkali metal binding affinity of the smallest and least polarizable amino acid, glycine (G), is the weakest of all 20 amino acids[3−5] and that glycine binds to Na^+ in a [N,CO] bidentate configuration[6,7] and to K^+ in a [COOH] bidentate binding mode at the carboxyl group.[8] In a few cases, this work has been expanded to small metalated peptides, such as glycylglycine (diglycine, GG) and glycylglycylglycine (triglycine, GGG). For instance, Kebarle and co-workers[9] carried out a threshold collision-induced dissociation (TCID) study of Na^+GG and reported a bond dissociation energy (BDE) of 179.5 ± 10 kJ/mol at 298 K. A similar value of 177 ± 10 kJ/mol was measured by Cerda et al.[10] using Cook's kinetic method[11,12] when nucleobases (adenine, cytosine, and guanine) were used as reference bases. Feng et al.[13] determined the dissociation free energies of the Na^+GG complex also using the kinetic method and reported a ΔG value of 143 kJ/mol at 350 K, which corresponds to a metal cation binding affinity (enthalpy) of about 186 kJ/mol at room temperature (calculated using ΔS_{350} and $(\Delta H_{350} - \Delta H_{298})$ values determined in the present study). The kinetic method was again used by Wesdemiotis and co-workers in the most recent measurements of Na^+ binding affinities at 298 K of GG[14] and GGG.[15] Here, amino acids and GG were used as reference bases, respectively, with values of 203 ± 8 and 237 ± 9 kJ/mol obtained, respectively, the former being 26 kJ/mol higher than their earlier measurements. This appreciable change was justified by good agreement of the experimental binding affinities of the sodium cation to the reference amino acids (measured by several different experimental methods[16−19]) and high-level theoretical values.[14−19]

Ab initio calculations of such systems also have been performed for GG,[10,20] GGG,[15,20−22] Li^+GG,[23] Na^+GG,[9,10,14,23,24] K^+GG,[25] and Na^+GGG.[15,24] In all cases, the metal cation was found to prefer a multidentate coordination with the functional groups of the peptide, as is discussed further below.

The present study was designed to provide absolute M^+ binding affinities for M^+GG and M^+GGG ($M^+ = Na^+$ and K^+) measured by TCID methods using a guided ion beam tandem mass spectrometer. Complementary ab initio calculations on M^+GG and M^+GGG ($M^+ = Li^+$, Na^+, and K^+) were performed for low-lying structures of these complexes and the free GG and GGG ligands at the B3LYP, B3P86, and MP2(full) levels using the 6-311+G(2d,2p) basis set with optimized structures and zero-point energies (ZPE) determined at the B3LYP/6-311+G(d) level. Thus, the present efforts complement the previous experimental studies of Na^+GG and Na^+GGG while resolving the conflicting values from previous work for Na^+GG and expanding their scope to a systematic evaluation of the simplest di- and tripeptide binding to potassium cations. The present theoretical efforts augment the experimental studies by providing needed molecular parameters as well as visualization of the processes investigated experimentally and allow a systematic examination of all three metalated GG and GGG systems. As compared to previous theoretical work, the present study extends the systems examined to Li^+GGG and K^+GGG, while also performing a more comprehensive examination of

10.1021/jp710709j CCC: $40.75
Published on Web 03/26/2008

the low-energy conformations of all systems. A key driving force for the present study was to evaluate whether TCID methods are capable of accurately measuring thermochemistry for biological molecules as large as a tripeptide. This is by no means clear given the large discrepancy between the TCID measurement of Kebarle and co-workers[9] on Na^+GG and the most recent value from kinetic method studies.[14]

2. Experimental and Computational Methods

2.1. General Experimental Procedures. The guided ion beam tandem mass spectrometer (GIBMS) used to measure the cross sections for TCID of the alkali metal cation GG and GGG complexes has been described previously in detail.[26,27] Briefly, ions are created in electrospray ionization (ESI) or dc discharge flow tube (DC/FT) sources (described next), extracted, focused, and accelerated through a magnetic momentum analyzer to select ions of interest. The mass selected ions are decelerated and injected into a radio frequency (rf) octopole ion beam guide, where ions are radially trapped.[28] The kinetic energy of the ions in the guide is controlled by the dc voltage applied to the octopole. The octopole passes through a gas cell of effective length 8.6 cm that contains the neutral reactant (Xe in the present experiments). All product and residual reactant ions drift to the end of the octopole where they are extracted and focused into a quadrupole mass filter for mass analysis. The ions are detected by a 27 kV conversion dynode-secondary electron scintillation detector[29] interfaced with fast pulse counting electronics. The raw ion intensities are converted to cross sections as described elsewhere.[26] The absolute cross sections are estimated to be accurate to ±20% with relative uncertainties of ±5%. Laboratory (lab) collision energies are converted to center-of-mass (CM) energies using the equation $E_{CM} = E_{lab}M/(M + m)$, where M and m are the reactant neutral and ion masses, respectively. All energies cited below are in the CM frame unless otherwise noted. The absolute energy scale and the corresponding full width at half-maximum (fwhm) of the ion beam kinetic energy distribution are determined by using the octopole as a retarding energy analyzer.[26] The energy spread is nearly Gaussian and has a typical fwhm of 0.1−0.2 eV (lab) for the ESI source and ~0.3 eV (lab) for the DC/FT source.

It has been shown previously[30] that the pressure of the neutral reactant can influence the shape and onset of TCID cross-sections because of the effects of multiple collisions. To obtain data free from pressure effects (i.e., at rigorously single-collision conditions), data are collected at about 0.04, 0.08, and 0.15 mTorr, and the cross sections are extrapolated to zero reactant pressure prior to threshold analysis. A complete set of pressure measurements was reproduced at least twice for each system. In the Na^+GGG system, we observed a noticeable Xe pressure dependence (where the apparent threshold shifts lower by ~0.4 eV as the pressure is increased). For all other primary cross sections, little pressure dependence is observed; however, secondary dissociation processes (e.g., elimination of the second ligand from Na^+G_2) exhibit a larger pressure dependence. This is mainly because of multiple energizing collisions that greatly enhance the dissociation probability especially near the threshold of these higher energy processes.

2.2. Electrospray Ionization Source. The M^+GG and M^+GGG complex ions of interest are formed by ESI in a source detailed elsewhere.[31] Briefly, ~10^{-4} M solutions were made by dissolving GG or GGG and MCl salt (M = Na or K) in pure HPLC grade water supplied by Mallinckrodt Chemicals. The MCl salt, GG, and GGG were purchased from Aldrich or Sigma and used as received. These solutions were introduced into the ESI needle by a syringe pump at a rate of 200−400 μL/h. The spraying needle was typically set at about 2 kV above ground, and the entrance to the ESI capillary was biased at 20−50 V relative to ground. The resulting ions enter the source chamber by passing through a 5 in. long, 0.020 in. inner diameter capillary. The capillary tubing is heated to about 80 °C for the purpose of drying the complexes, thereby removing solvent molecules. Typical pressures in the source chamber during operation are about 0.3 Torr. Ions exiting the capillary enter a rf ion funnel,[32,33] which collects the ions and focuses them. The ions are then injected into a hexapole ion guide where they undergo enough collisions to be thermalized to 300 K both vibrationally and rotationally, as demonstrated previously.[31] Ions exiting the hexapole are then extracted by dc ion optics and focused into the guided ion beam mass spectrometer.

2.3. dc Discharge Flow Tube Ion Source. The dc discharge flow tube (DC/FT) source serves as an alternative source of ions that has been used in this laboratory over the past 15 years and has been demonstrated to produce thermalized complex ions.[8,31,34−40] For comparison purposes, TCID experiments of Na^+G_2 and Na^+GG formed using the DC/FT source were performed. Briefly, sodium cations are generated at the head of a 1 m long flow tube using a continuous dc discharge with typical operating conditions of 1.4−2.0 kV and 15−25 mA. The sodium cations are carried down the flow tube by a buffer gas (ca. 10% argon in helium) at a flow rate of 5000−7000 sccm, with normal operating pressures of 0.3−0.4 Torr. About 50 cm downstream from the discharge, the neutral ligand is introduced into the flow tube using a temperature controlled probe, which is heated to about 170 °C for G and GG. The complex ions of interest are formed via three-body associative reactions of Na^+ with the ligand in the flow of the He/Ar carrier gas. The complex ions are thermalized to 300 K (the temperature of the flow tube) both vibrationally and rotationally by undergoing ~10^5 collisions with the buffer gases as they drift along the 1 m long flow tube.[8,31,34−40]

2.4. Threshold Analysis. For endothermic reactions, the threshold energies can be extracted by fitting the energy dependent cross sections in the threshold region using eq 1

$$\sigma(E) = \sigma_0 \sum_i g_i(E + E_i - E_0)^n/E \qquad (1)$$

where σ_0 is an adjustable parameter that is energy independent, n is an adjustable parameter that describes the energy deposition efficiency during collision,[27] E is the relative kinetic energy, and E_0 represents the CID threshold energy at 0 K. E_i are the internal energies of the rovibrational states i of the reactant ion with populations g_i, where $\Sigma g_i = 1$, such that $E + E_i$ is the total energy available to the colliding reactants. Vibrational frequencies and rotational constants used to calculate E_i and g_i are obtained from the calculations outlined in the next section. The Beyer−Swinehart algorithm[41] is used to evaluate the density of the rovibrational states, and the relative populations g_i are calculated for a Maxwell−Boltzmann distribution at 300 K.

Because the metal−ligand complexes investigated here are relatively large (10 heavy atoms for M^+GG and 14 heavy atoms for M^+GGG), it is critical to include unimolecular dissociation kinetics in the analysis of the CID cross sections. The time available for dissociation in the instrument used here is ~5×10^{-4} s (as previously measured by time-of-flight studies).[27] If this is insufficient for the complex ions to dissociate, then products will not be observed until a higher energy than the true CID threshold, leading to a kinetic shift. These kinetic shifts are estimated by the incorporation of RRKM theory into eq 1,

as described in detail elsewhere,[42,43] which transforms eq 1 into eq 2

$$\sigma_j(E) = (n\sigma_{0,j}/E)\Sigma g_i \int_{E_{0,j}-E_i}^{E} [k_j(E^*)/k_{\mathrm{tot}}(E^*)] \times \{1 - e^{-k_{\mathrm{tot}}(E^*)\tau}\}(E-\epsilon)^{n-1}\mathrm{d}(\epsilon) \quad (2)$$

Here, ϵ is the energy transferred from translation into internal energy of the complex during the collision, τ is the experimental time available for dissociation, and E^* is the internal energy of the energized molecule (EM) after the collision (i.e., $E^* = \epsilon + E_i$, with n, g_i, E_i, and E defined previously). The term $k_j(E^*)$ is the unimolecular rate constant for dissociation of the EM to channel j with threshold energy $E_{0,j}$ and scaling factor $\sigma_{0,j}$. The rate constants are defined by Rice−Ramsperger−Kassel−Marcus (RRKM) theory[44−46] in eq 3

$$k_{\mathrm{tot}}(E^*) = \sum k_j(E^*) = \sum d_j N^{\dagger}_{j,\mathrm{vr}}(E^* - E_{0,j})/h\rho_{\mathrm{vr}}(E^*) \quad (3)$$

where d_j is the reaction degeneracy for channel j, h is Planck's constant, $N^{\dagger}_{j,\mathrm{vr}}(E^* - E_{0,j})$ is the sum of rovibrational states of the transition state (TS) at an energy $E^* - E_{0,j}$ for channel j, and $\rho_{\mathrm{vr}}(E^*)$ is the density of rovibrational states of the EM at the available energy, E^*. In the limit that $k_{\mathrm{tot}}(E^*)$ is faster than the time-of-flight of the ions, the integration in eq 2 recovers eq 1.

To evaluate the rate constants in eq 3, vibrational frequencies and rotational constants for the EM and all TSs are required. Because the metal−ligand interactions in the complexes studied here are mainly long-range electrostatic interactions (ion−dipole, ion−quadrupole, and ion-induced dipole interactions), the most appropriate model for the TS is generally a loose association of the ion and neutral ligand fragments,[6,8,37,47−49] even for multidentate ligands.[50−52] This assumption was tested further in the present work. Therefore, the TSs are treated as product-like, such that the TS frequencies are those of the dissociated products. The transitional frequencies are treated as rotors, a treatment that corresponds to a phase space limit (PSL), as described in detail elsewhere.[42,43] For M^+L complexes dissociating to $M^+ + L$, the three transitional mode rotors have rotational constants equal to those of the ligand product. The 2-D external rotations are treated adiabatically but with centrifugal effects included.[53] In the present work, the adiabatic 2-D rotational energy is treated using a statistical distribution with an explicit summation over all possible values of the rotational quantum number.[42]

Before being compared to the experimental data, the calculated cross section is convoluted over the kinetic energy distribution of the ion beam and thermal energy distribution of the neutral collision gas (Doppler broadening), as described elsewhere.[26] A nonlinear least-squares analysis is used to provide optimized values for $\sigma_{0,j}$, $E_{0,j}$, and n. The uncertainty associated with $E_{0,j}$ is estimated from the range of threshold values determined from different data sets with variations of vibrational frequencies (±10% for most vibrations and a factor of 2 for the $M^+ - L$ modes) and the parameter n, variations in τ by a factor of 2, and the uncertainty in the absolute energy scale, 0.05 eV (lab).

In deriving the final optimized BDEs at 0 K, two assumptions are made. First, there is no activation barrier in excess of the endothermicity for the loss of ligands, which is generally true for ion−molecule reactions, especially the heterolytic noncovalent bond cleavages considered here.[54] Second, the measured threshold is assumed to correspond to dissociation of the ground state reactant to ground state ion and neutral ligand products. Given the relatively long experimental time frame available (~5×10^{-4} s), we assume that the dissociating products are able to rearrange to their ground state conformations upon dissociation. The appropriateness of this assumption for the complicated GG and GGG ligands is essentially verified by the good agreement between our experimental results with both theoretical and literature values.

2.5. Computational Details. A simulated annealing procedure[6] using the AMBER forcefield based on molecular mechanics[55] was used to search for possible stable structures in each system's conformational space. All possible structures identified in this way were further optimized using NWChem[56] at the HF/3-21G level.[57,58] Unique structures for each system within about 50 kJ/mol of the lowest energy structure (about 50 for each complex) were further optimized using Gaussian 03[59] at the B3LYP/6-31G(d) level[60−62] with the "loose" keyword (maximum step size of 0.01 au and an rms force of 0.0017 au) to facilitate rapid convergence. The 10−15 lowest energy structures obtained from this procedure were then chosen for higher level geometry optimizations and frequency calculations using density functional theory (DFT) at the B3LYP/6-311+G(d) level.[63,64] This level of theory has been shown to be adequate for accurate structural descriptions of comparable metal−ligand systems.[6,8] Single-point energy calculations were carried out for the lowest six to 15 optimized structures at the B3LYP, B3P86, and MP2-(full) levels using the 6-311+G(2d,2p) basis set. ZPE corrections were determined using vibrational frequencies calculated at the B3LYP/6-311+G(d) level after scaling by 0.9804.[65] Basis set superposition errors (BSSE) in all bond dissociation energy calculations were estimated using the full counterpoise method.[59,66] Previous work[6,8,49,67,68] has indicated that BSSE corrections on alkali metal systems are generally small for DFT calculations, and we found this to be true here as well. Both B3LYP and B3P86 calculations have BSSE corrections of 1−3 kJ/mol, whereas the MP2(full) values have BSSE corrections of 4−14 kJ/mol.

3. Results

3.1. Cross Sections for Collision-Induced Dissociation. Experimental cross sections were obtained for the interaction of Xe with M^+L, where $M^+ = Na^+$ and K^+ and L = GG and GGG, as a function of collision energy. Figures 1 and 2 show representative data for CID of M^+GG and M^+GGG complexes, respectively, formed in the ESI source. Over the energy ranges examined, the loss of the intact peptide, eq 4, is seen in all four M^+L systems

$$M^+L + Xe \rightarrow M^+ + L + Xe \quad (4)$$

The magnitudes of the cross sections for losing GG and GGG from M^+L are comparable to one another in all cases: 10−30 $\times 10^{-16}$ cm^2 at high energies. The magnitudes of the K^+ cross sections are larger than those for Na^+, which reflect the fact that the K^+L complexes have thresholds that are ~1 eV smaller than those of Na^+L. This is consistent with previous threshold CID bond dissociation energy measurements of metallized amino acids[6,8,19,69] and many other ligands.[70] Finally, the apparent thresholds of M^+GGG for each metal are clearly larger than those of M^+GG, demonstrating that the extra glycyl group in GGG does bond to the metal cation. In no system was a ligand exchange process forming an ion containing Xe observed.

CID of Na^+GGG, Figure 2b, shows an additional fragmentation process in which a peptide bond is broken with a hydrogen

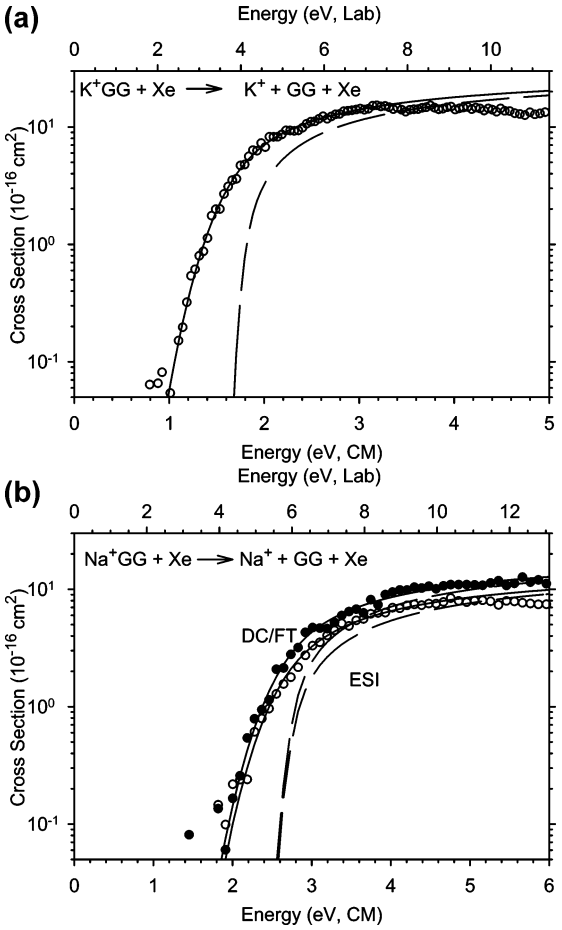

Figure 1. Zero pressure extrapolated cross sections for CID of K^+GG (a) formed in the electrospray ionization (ESI) source and Na^+GG (b) formed in the ESI (open symbols) and dc discharge flow tube (DC/FT, solid symbols) sources with Xe as a function of kinetic energy in the center-of-mass (lower *x*-axis) and laboratory (upper *x*-axis) frames. The solid lines show the model cross sections of eq 2 convoluted over the neutral and ion kinetic and internal energies. The dashed lines show the model cross sections in the absence of experimental energy broadening for reactants with an internal energy of 0 K.

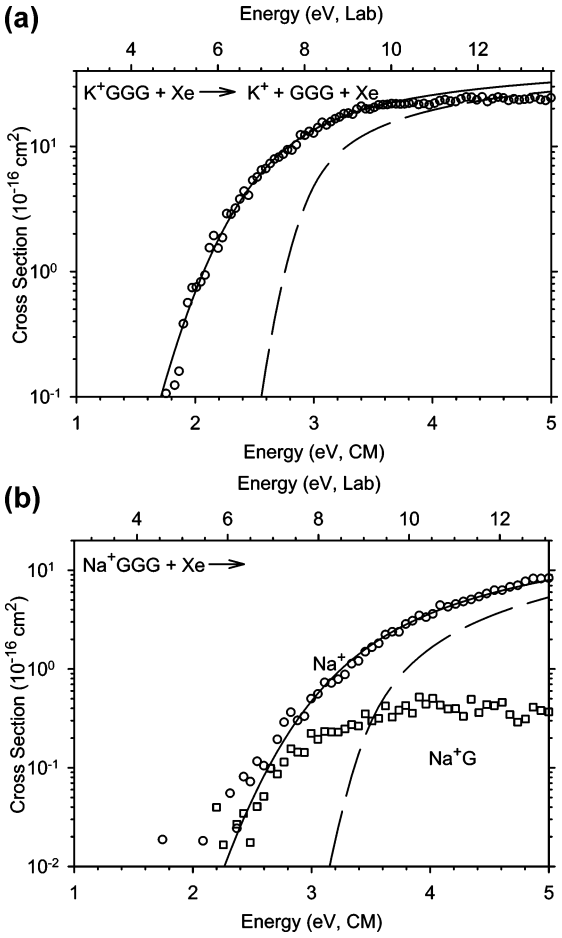

Figure 2. Zero pressure extrapolated cross section for CID of K^+GGG (a) and Na^+GGG (b) formed in the electrospray ionization source with Xe as a function of kinetic energy in the center-of-mass (lower *x*-axis) and laboratory (upper *x*-axis) frames. The solid lines show the model cross sections of eq 2 convoluted over the neutral and ion kinetic and internal energies. The dashed lines show the model cross sections in the absence of experimental energy broadening for reactants with an internal energy of 0 K.

being transferred internally to produce the Na^+G ion and neutral [GG − H_2O], eq 5

$$Na^+GGG + Xe \rightarrow Na^+G + [GG - H_2O] + Xe \quad (5)$$

Formation of product ions from alternate decomposition pathways, such as Na^+GG and Na^+[GG − H_2O], were not observed in a mass scan of potential products and therefore must have magnitudes below $\sim 10^{-17}$ cm^2. The fragmentation process (eq 5) presumably involves passing over one or more transition states. The requisite computations involved in properly analyzing the threshold for this process are sufficiently complicated that this line of research is pursued elsewhere.[71] The cross section for eq 4 is over 1 order of magnitude larger than that for eq 5, indicating that the effect of competition on the threshold for eq 4 is small and can therefore be ignored in the modeling of the primary decomposition reaction, as confirmed by an analysis that does include competitive modeling of both reactions.[71]

Figure 1b shows that the experimental cross sections for CID of Na^+GG formed using the DC/FT and ESI ion sources have the same energy dependence and differ only in magnitude by ∼10%, well within the 20% absolute uncertainty of these measurements. This demonstrates that both sources produce thermalized complexes. Figure 3 shows the CID cross sections for the bis-ligated Na^+G_2 complex formed in the DC/FT source. In contrast to Na^+GG, Figure 1b, this complex easily loses G at low energies, eq 6, consistent with two ligands both coordinated to the sodium cation

$$Na^+G_2 + Xe \rightarrow Na^+G + G + Xe \quad (6)$$

Subsequent loss of the second ligand to form Na^+ is also seen ∼2 eV higher in energy. In this system, the magnitude of the total cross section is larger than the M^+GG and M^+GGG systems. This is consistent with the fact that the apparent threshold for losing G from Na^+G_2 is much smaller (by at least 1 eV) than that for losing the peptide from Na^+L, where L = GG and GGG.

3.2. Threshold Analysis and Results. Peptide and glycine losses in eqs 4 and 6 were modeled using eq 2. Formation of Na^+ from Na^+G_2 (sequential loss of glycine ligands) was also modeled using a recent extension of eq 2 that uses statistical methods to predict the kinetic shifts inherent in such a sequential process.[72] Figures 1−3 show that the experimental cross sections are reproduced well by eq 2 over extended energy and magnitude ranges. The optimized parameters of eq 2 for all systems using molecular parameters for the ground state complexes and PSL transition states calculated at the B3LYP/

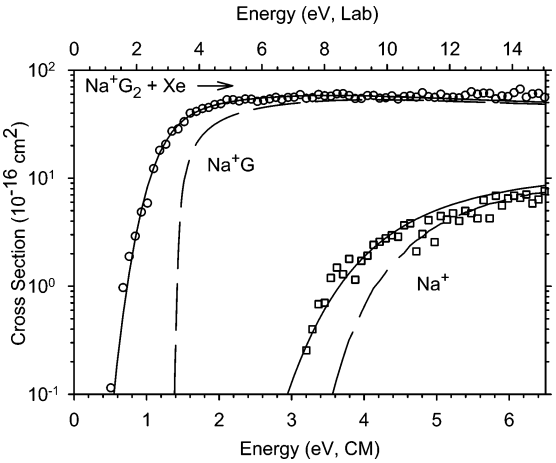

Figure 3. Zero pressure extrapolated cross sections for CID of Na^+G_2 formed in the flow tube source with Xe as a function of kinetic energy in the center-of-mass (lower *x*-axis) and laboratory (upper *x*-axis) frames. The solid line shows the model cross sections convoluted over the neutral and ion kinetic and internal energies. The dashed line shows the model cross sections in the absence of experimental energy broadening for reactants with an internal energy of 0 K.

6-311+G(d) level (see next section) are reported in Table 1, including threshold values with and without RRKM lifetime analysis.

The kinetic shifts for M^+GG and M^+GGG are 0.44 and 1.18 eV in the case of Na^+ and 0.21 and 0.81 eV in the case of K^+, respectively. The kinetic shift for losing glycine from Na^+G_2 is smaller, 0.14 eV. Kinetic shifts for CID of Na^+G and K^+G were previously found to be only 0.04 and 0.01 eV, respectively.[6,8] The size of the kinetic shift varies such that higher E_0 values and larger neutral fragments yield larger kinetic shifts. The relatively large kinetic shift values found here indicate the importance of incorporating RRKM theory into the threshold analysis when dealing with such complex systems.

Table 1 also includes the analysis of our Na^+GG data using molecular parameters taken from Klassen et al.[9] as calculated using AM1 semiempirical methods. They used a similar TCID approach to measure this threshold but analyzed the data using a tighter TS assumption to account for the kinetic shift, which differs from the loose PSL TS assumption used in the present studies. Their protocol for estimating the molecular parameters of the TS was to drop one of the three lowest vibrational frequencies and to set the other two to either 10 cm^{-1} (their preferred approach) or 30 cm^{-1}. These tighter TS parameters lead to a much larger kinetic shift and lower threshold (by 0.33 eV) than the loose PSL TS parameters. Both Kebarle and coworkers[9] and we agree that there is no reason why dissociation of the Na^+GG complex should require a truly tight TS because the long-range interaction between Na^+ and GG is attractive; however, the empirical approach used by the previous workers leads to a substantially tighter TS as compared to the PSL TS, the loosest possible TS. Comparison of these disparate threshold values with previous experiments and theory will be used to determine the most accurate approach.

Table 1 also includes $\Delta S^{\dagger}_{1000}$ values, which reflect the looseness of the transition states. In all cases, the $\Delta S^{\dagger}$ values for losing intact ligands are 30−50 J/mol K, which is consistent with the assumption of loose transition states for the M^+GG, M^+GGG, and Na^+G_2 systems. It is noteworthy that the $\Delta S^{\dagger}_{1000}$ value is negative for Na^+GG using the molecular parameters of Klassen et al. that produced their best results, which reflects the tighter TS assumption for dissociation.

3.3. Theoretical Results. Our detailed theoretical results for conformations of GG, GGG, and their metalated complexes can be found in the Supporting Information. Relative energies of the GG and GGG ligands are included in Table S1, and those for their metalated complexes are found in Table S2 of the Supporting Information. Some useful geometric parameters of these species are included in Table S3. Detailed structural information for G, Na^+G, and K^+G can be found elsewhere.[6,8,73,74] Our current exploration of the GG and GGG conformational spaces using the protocol outlined previously reproduces results of previous work[10,15,20−22,25] but also identifies more low-energy conformations than earlier studies. We find that N-ctt is predicted to be the ground state (GS) structure at the B3LYP level of theory, whereas N-cgg is the GS conformer calculated by B3P86, and MP2(full) finds these conformers to be isoenergetic (Table S1). At all levels of theory, both structures lie within 3 kJ/mol of one another, as does N-cgt, which is almost identical to N-ctt except that the carbonyl carbons are gauche instead of trans to each other (ϕ_2 in Table S3). N-ctt was found to be the GS structure at the HF/6-31G(d) level by Cerda et al. (who did not consider N-cgg or N-cgt),[10] whereas Shoeib et al.[20] found that N-cgg is the most stable structure at the B3LYP/DZVP level (but did not consider N-ctt or N-cgt). For GGG, our calculations at three different levels predict N-cgggt to be the GS structure, as previously reported by Shoeib et al.,[20] Strittmatter and Williams,[21] Zhang et al.,[22] and Wang et al.,[15] although these reports did not elucidate all the alternate conformations presented in the Supporting Information.

Results of the present calculations for metalated peptides along with those found in the literature are detailed in the Supporting Information. As described above, calculations for $M^+ = Li^+$ are included for comparison purposes and allow a more systematic study of the periodic trends in these systems. Our independent conformational searches using the protocol mentioned previously for M^+GG and M^+GGG systems reproduce most of the findings in the literature for M^+GG and Na^+GGG (as indicated by similar relative energies in Table

TABLE 1: Fitting Parameters for Eq 2 and Entropies of Activation at 1000 K[a]

reactant (ion source)	ionic product	σ_0[b]	n[b]	E_0[c] (eV)	E_0[d] (PSL) (eV)	$\Delta S^{\dagger}_{1000}$ (J/mol K)
Na^+GG (ESI)	Na^+	22 (5)	1.0 (0.2)	2.61 (0.14)	2.17 (0.14)	50 (14)
Na^+GG (FT)	Na^+	22 (5)	1.1 (0. 2)	2.60 (0.14)	2.17 (0.14)	50 (14)
Na^+GG (ESI)	Na^+[e]	23 (5)	1.1 (0.2)	2.64 (0.15)	1.84 (0.14)	−3 (6)
Na^+GGG (ESI)	Na^+	17 (4)	1.5 (0.2)	3.67 (0.17)	2.49 (0.18)	49 (23)
Na^+G_2 (FT)	Na^+G	104 (4)	0.8 (0.1)	1.44 (0.09)	1.30 (0.10)	34 (2)
	Na^+[f]	28 (6)	0.8 (0.1)		2.90 (0.10)	
K^+GG (ESI)	K^+	41 (16)	1.1 (0.2)	1.75 (0.08)	1.54 (0.08)	38 (13)
K^+GGG (ESI)	K^+	54 (20)	0.9 (0.1)	2.71 (0.14)	1.90 (0.16)	43 (22)

[a] Uncertainties are in parentheses. [b] Values obtained including lifetime effects. Similar values were obtained when lifetime effects were excluded. [c] No lifetime effect. [d] With lifetime effects included using a phase space limit (PSL) transition state. [e] Data modeled using the TS molecular parameters from ref 9. [f] Sequential channel fitting results.

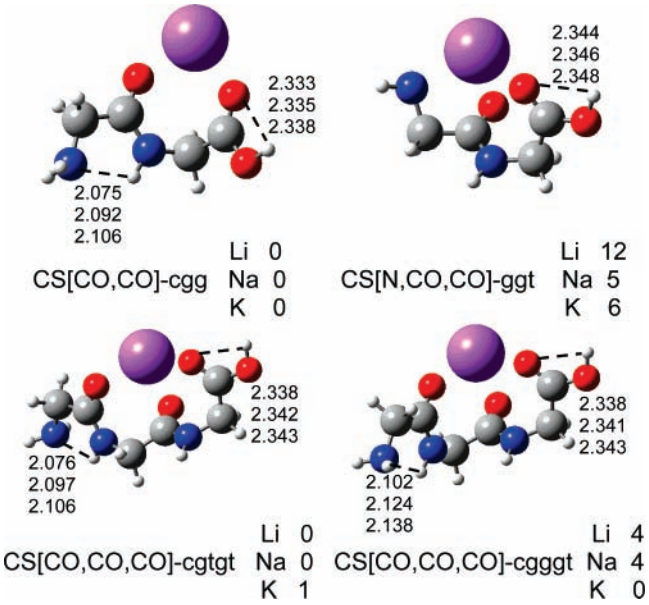

Figure 4. Two lowest energy structures of Na^+GG and Na^+GGG calculated at the B3LYP/6-311+G(d) level of theory. Relative energies (kJ/mol) of M^+GG and M^+GGG ($M^+ = Li^+$, Na^+, and K^+) calculated at the B3LYP/6-311+G(2d,2p) level of theory including ZPE corrections also are indicated. Dashed lines show hydrogen bonds with their bond lengths in angstroms for all three metal ions.

S2).[9,10,14,15,23−25] In addition, we located several alternative conformations in all cases and examined Li^+GGG and K^+GGG for the first time. The lowest two energy structures for M^+GG and M^+GGG are shown in Figure 4.

The three levels of theory used in the present calculations predict that the most favorable sites to bind a metal cation to GG are the two carbonyl oxygen atoms without, CS[CO,CO]-cgg, or with, CS[N,CO,CO]-ggt, the amino nitrogen (Figure 4). Previous work on the Na^+GG complex also has located the bidentate[9,10,23,24] or tridentate structure[14] as the GS. Additionally, the bidentate CS[CO,CO]-cgg structure was found to be the most stable structure for Li^+GG by Benzakour et al.[23] and for K^+GG by Wong et al.[25] Our work shows that DFT calculations prefer the bidentate CS[CO,CO]-cgg structure, whereas MP2 calculations find that the CS[N,CO,CO]-ggt structure is relatively more stable.

For M^+GGG, all levels of theory examined here indicate that the GS structure for Li^+GGG is CS[CO,CO,CO]-cgtgt and that for K^+GGG is CS[CO,CO,CO]-cgggt. For Na^+GGG, the former conformer is favored by the DFT calculations and the latter by MP2(full). These results reproduce those for Na^+GGG of Wyttenbach et al.[76] at the B3LYP/6-31G level (no ZPE corrections) and Wang et al.[15] at the MP2(full)/6-311+G(2d,-2p)//HF/6-31G(d) level (Table S2). The levels of theory considered here show that the two CS[CO,CO,CO] tridentate structures are within 6 kJ/mol of each other, consistent with their very similar structures (Figure 4) differing primarily in the ψ_2 angle (Table S3). Activation energies including ZPE for interconversion between these conformers (relative to cgggt) were calculated to be 10−11, 17−21, and 22−28 kJ/mol for Li^+, Na^+, and K^+, respectively.

3.4. Na^+G_2. The lowest energy conformer for Na^+G_2 has a tetradentate binding configuration in which both glycine molecules bind to Na^+ with configurations similar to the M1[N,CO] conformation of Na^+G.[6] The glycine ligands are distributed on opposite sides of Na^+ with the backbone planes of glycine almost perpendicular to each other. The Na^+−O and Na^+−N distances are 2.30 and 2.50 Å, respectively, slightly larger than the corresponding distances of 2.26 and 2.44 Å for Na^+G.[6]

4. Discussion

4.1. Conversion from 0 to 298 K. Conversion from 0 K BDEs to 298 K bond enthalpies and free energies is accomplished using rigid rotor/harmonic oscillator approximations and frequencies calculated at the B3LYP/6-311+G(d) level. These ΔH_{298} and ΔG_{298} values along with the conversion factors and 0 K enthalpies measured here are reported in Table 2. The uncertainties listed are determined by scaling all of the vibrational frequencies by ±10% except for the metal−ligand frequencies, where 2-fold variations are applied, and by using various sets of frequencies from any conformer that is within 5 kJ/mol of the GS structure. Relative ΔH_{298} and ΔG_{298} values are similar to the 0 K values because $\Delta H_{298} - \Delta H_0$ values are small and all $T\Delta S_{298}$ values are similar.

4.2. Trends in Experimental BDEs. Our results for the energies required to remove the intact ligand from M^+L, where $M^+ = Na^+$ and K^+ and L = GG and GGG, are listed in Table 3, along with TCID values from our laboratory for L = G.[6,8] The BDEs decrease from Na^+ to K^+ because the electrostatic interaction decreases with the increasing bond distances resulting from the increasing size of the metal cation (0.98 and 1.33 Å, respectively[77]). A similar trend is found for the M^+G systems, as well as other ligands.[69,70] The BDEs follow the order G < GG < GGG for both alkali metal cations investigated here, consistent with the increasing number of carbonyls in the ligands. The BDEs for Na^+ and K^+ increase by 45 and 28 kJ/mol as the number of residues increases from G to GG and 31 and 34 kJ/mol from GG to GGG, respectively. Note that these changes are much less than half those for binding G (82 and 60 kJ/mol for Na^+ and K^+, respectively) or even half the second G ligand (62 kJ/mol for Na^+). These differences can be attributed to the steric constraints and increased electron delocalization associated with binding the longer peptide chains to the metal cations.

Previous TCID experiments of metalated amino acids suggest that the BDEs of amino acids to alkali metal cations can be correlated with the polarizabilities of the neutral ligands.[19,69] This is found to be the case for these small peptides as well. The BDEs of the current systems combined with previous experimental values for the M^+G systems[6,8] are plotted against the polarizabilities of G, GG, and GGG in Figure 5. Isotropic

TABLE 2: Enthalpies and Free Energies of GG and GGG Binding (kJ/mol) to Na^+ and K^+ at 0 and 298 K

complex	ionic product	ΔH_0[a]	$\Delta H_{298} - \Delta H_0$[b]	ΔH_{298}	$T\Delta S_{298}$[b]	ΔG_{298}
Na^+GG	Na^+	209 (13)	2.5 (1.7)	211 (13)	36.9 (5.5)	176 (14)
Na^+GGG	Na^+	240 (17)	1.0 (1.5)	241 (17)	33.3 (4.8)	208 (18)
K^+GG	K^+	149 (7)	1.8 (1.0)	150 (7)	35.3 (5.0)	115 (9)
K^+GGG	K^+	183 (15)	0.5 (3.4)	183 (16)	33.6 (13.8)	150 (21)
Na^+G_2	Na^+G	125 (10)	−1.5 (0.6)	124 (10)	38.3 (7.4)	86 (12)

[a] Experimental values from this work (Table 1). [b] Values were computed using standard formulas and molecular constants calculated at the B3LYP/6-311+G(d) level.

TABLE 3: G, GG, and GGG Binding Energies (kJ/mol) to Na^+ and K^+ at 0 K

	experiment		theory				
bond	TCID[a]	literature[b]	B3LYP[c]	B3P86[c]	MP2(full)[c]	MP2(full)[d]	literature
Na^+-G	164 (6)[e]	151 (10)[f]	163.1	158.1	151.1	160.1	
		166 (25)[g]					
Na^+-GG	209 (13)	179 (10)[f]	201.8	195.9	188.5	198.6	208.5[h]
		175 (10)[i]					190.0[j]
		184 (16)[k]					199.5[l]
		201 (8)[m]					
Na^+-GGG	240 (17)	236 (9)[n]	248.6	237.9	224.3	238.7	242[o]
			247.6[p]	237.8[p]	224.6[p]	238.9[p]	
			250.9[q]	240.1[q]	228.4[q]	243.0[q]	
GNa^+-G	125 (10)		116.5	113.1	113.1	125.7	
K^+-G	121 (4)[r]	125 (10)[f]	115.9	118.6	113.5	117.3	
K^+-GG	149 (7)		143.1	141.6	139.5	145.2	151.8[s]
K^+-GGG	183 (15)		182.8	181.0	178.0	186.2	
MAD[t]			5 (3)	6 (5)	12 (5)	4 (3)	

[a] Present results, threshold collision-induced dissociation. [b] Values at other temperatures were converted to 0 K using vibrational frequencies calculated at the B3LYP/6-311+G(d) level (Table 2). [c] Present values. Energies calculated at the corresponding 6-311+G(2d,2p)//B3LYP/6-311+G(d) level including ZPEs and BSSE corrections. [d] Same as footnote c excluding BSSE corrections. [e] TCID, ref 6. [f] TCID, ref 9. [g] Kinetic method, ref 81 as adjusted in ref 82. [h] B3LYP/6-31++G(d,p) with ZPE corrections included, ref 23. [i] Kinetic method, ref 10. [j] MP2(full)/6-311+G(2d,2p)//HF/6-31G(d) with BSSE correction, ref 10. [k] Kinetic method, ref 13. [l] MP2(full)/6-311+G(2d,2p)//MP2(full)/6-31G(d) without BSSE correction, ref 14. [m] Kinetic method, ref 14. [n] Kinetic method relative to D (Na^+GG) = 201 kJ/mol, ref 15. [o] MP2(full)/6-311+G(2d,2p)//HF/6-31G(d), ref 15. [p] Structures and ZPE calculated at the B3LYP/6-311++G(2d,2p) level. All single-point energies are calculated as in footnote a. [q] Structures and ZPEcalculated at the MP2(full)/6-31+G(d) level. All single-point energies are calculated as in footnote a. [r] TCID, ref 8. [s] B3LYP/6-311+G(3df,2p)//B3LYP/6-31G(d) with a 0.8929 scaling factor used for ZPE corrections calculated at the HF/6-31G(d) level, ref 25. [t] Mean absolute deviation from the present experimental values.

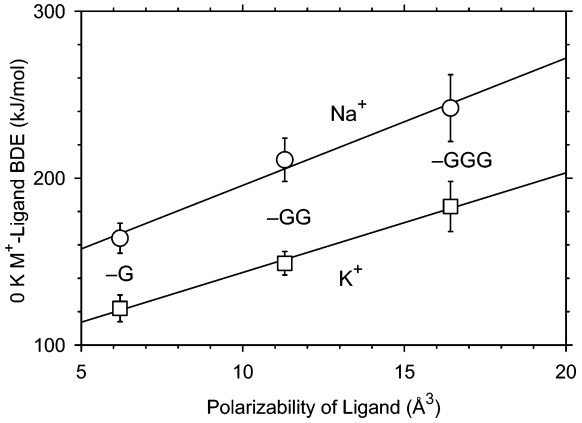

Figure 5. Experimental 0 K BDEs of M^+L vs the theoretical molecular polarizability of L, where L = G, GG, and GGG and $M^+ = Na^+$ and K^+.

molecular polarizabilities of 6.16, 11.30, and 16.20 Å^3 were calculated at the PBE0/6-311+G(2d,2p) level of theory using the B3LYP/6-311+G(d) optimized geometries (values for the free ligands and frozen structures from the metalated complexes were essentially identical, differing by less than 2%). This level of theory has been shown to provide polarizabilities that are in good agreement with measured values.[78] The good linear relationship in Figure 5 suggests that the polarizabilities of the neutrals play a key role in the binding strength of these systems, although a similar correlation is obtained with the number of carbonyl sites. It should be noted that neither correlation passes through zero and that the present polarizability correlation with G, GG, and GGG differs from that obtained previously for G, P, M, F, Y, and W.[19,69] The theoretical study of the K^+GG system by Wong et al.[25] finds that K^+ is closely aligned with the molecular dipole vector of GG in every low-lying potassiated diglycine structure. These authors conclude that the ion−dipole interaction is important in the binding of the metal cation and peptide. We also find that the dipole moments of the complexed ligands are pointed toward the metal ion in these complexes, although it is interesting that the BDEs do not correlate with the calculated dipole moments of the G, GG, and GGG ligands in their ground state complexed geometries (3.15, 5.85, and 5.22 D for Na^+, respectively, and 6.20, 5.89, and 7.78 D for K^+, respectively). This simply demonstrates that the final bond energies of molecules as complex as peptides are a superposition of electrostatic and steric effects.

The 0 K BDEs for losing GG from K^+GG and Na^+GG are slightly larger (by ~5 and 10 kJ/mol, respectively) than those of the corresponding serine (S) and threonine (T) systems also investigated in our lab.[79] This correspondence is consistent with the observation that GG interacts with the metal cation in a similar tridentate fashion as S and T. In addition, kinetic shifts for K^+GG and Na^+GG are slightly larger (by ~10 kJ/mol) than those in the corresponding M^+T systems, consistent with the fact that GG has one more heavy atom (and one less H atom) and slightly larger experimental E_0 values than T.

The BDE of a second G ligand to Na^+ has not been measured previously; however, it has been pointed out that the binding energy of G to Na^+ is comparable to the sum of the first and second water binding energies to Na^+: 164 ± 6[6] kJ/mol versus 177 ± 10 kJ/mol,[80] respectively. Here, we find that the second G ligand has the same binding energy (125 ± 10 kJ/mol) to Na^+ as the sum of the third and fourth water molecules bound to Na^+ in the $Na^+(H_2O)_4$ complex: 125 ± 9 kJ/mol.[80] These correspondences suggest that the first and second G both interact with Na^+ in a bidentate [N,CO] configuration, consistent with theory. In addition, statistical modeling of the sequential elimination of both G ligands from Na^+G_2 in the present work gives a threshold of 280 ± 10 kJ/mol (Table 1), which agrees very well with the summation (289 ± 12 kJ/mol) of the first (164 ± 6 kJ/mol, ref 6) and second (125 ± 10 kJ/mol, Table 3) BDEs between G and Na^+. This correspondence indicates that the sequential dissociation of such a large molecular system involving loose transition states can be modeled statistically[72] to obtain accurate thermodynamic information.

4.3. Comparison of Experimental BDEs with Literature Values. Previously measured BDEs for the M^+L complexes, where $M^+ = Na^+$ and K^+ and L = GG and GGG, are compared to the present experimental values in Table 3. For accurate

comparison with the present TCID results, all literature values are converted to 0 K values using the needed molecular parameters calculated at the B3LYP/6-311+G(d) level (Table 2).

Using a TCID approach, Klassen et al.[9] reported the BDE of the Na^+GG complex to be 179.5 ± 10 kJ/mol at 298 K (corresponding to 179 ± 10 kJ/mol at 0 K if their tighter TS parameters are used for thermal corrections). This value lies well below the value obtained in these experiments where a loose PSL TS is assumed. By modeling our own data using the tighter TS parameters of Klassen et al.,[9] it can be demonstrated that the difference between the two BDEs is exclusively a result of the TS assumptions made (Table 1). Kish et al.[14] suggested that the low value from Klassen et al. was a result of incomplete thermalization of the Na^+GG precursor ion, but the present results demonstrate that this suggestion is incorrect. As demonstrated in the following discussion, the good agreement of the present TCID results with the most recent values in the literature demonstrates that the loose PSL TS assumption is more appropriate for analyzing the CID of such systems.

Cerda et al.[10] measured the Na^+ binding affinity of GG using the extended kinetic method and obtained a value corresponding to 175 ± 10 kJ/mol at 0 K, in good agreement with Klassen et al.[9] The same group later argued[14] that this value is underestimated because the reference bases used were rigid and planar nucleobases (adenine, cytosine, and guanine), which could force GG to interact with Na^+ in a monodentate configuration, thereby leading to an excited conformation upon dissociation. Also, the large $\Delta(\Delta S_{Na})$ value (27 J/mol K) obtained could indicate another source of error. The Na^+GG system was reinvestigated by the same laboratory again using the kinetic method but with amino acids, serine (S), proline (P), threonine (T), and phenylalanine (F), as reference bases. A new value of 203 ± 8 kJ/mol at 298 K (corresponding to 201 ± 8 kJ/mol at 0 K (Table 3)) was obtained. This new measurement agrees well with the value from the present TCID study. It is noteworthy that the amino acids chosen as reference bases bind Na^+ as tridentate ligands,[16,17,19,49,79] except for P, which is bidentate.[40] In addition, these studies show that S, T, and F have similar binding energies to Na^+. Further, GG has one more heavy atom but one less H atom than T and P. These factors (similar binding configuration and number of heavy atoms) imply that the entropy effects, $\Delta(\Delta S_{Na})$, upon dissociation could largely cancel, therefore producing reasonable ΔH values from the kinetic method. However, it is perhaps questionable as to whether the amino acid (X) ligands (S, T, and F) used as references can bind in tridentate configurations to Na^+GG because of steric effects, which could mean that dissociations of the XNa^+GG complexes investigated may not yield the ground state conformations. Thermochemistry that would appear to be reasonable might still be obtained in such a situation if both the Na^+GG and the Na^+X products were formed in excited bidentate configurations, but the relative energies determined could vary from those of the ground states.

Feng et al.[13] measured the free energy (ΔG) for dissociation of Na^+GG using the kinetic method and reported a value of 143 ± 16 kJ/mol at the estimated effective ion temperature of 350 K in an ion trap. A 0 K enthalpy value (ΔH_0) of 184 ± 16 kJ/mol deduced using a ΔS_{350} value calculated here (124 J/mol K) is included in Table 3. This value is somewhat lower than the present values of 209 ± 13 kJ/mol for Na^+GG and 201 ± 8 kJ/mol from Kish et al.[14] There are several possible reasons for the discrepancy. The most likely of these is that the absolute anchor used for these results is in error. Indeed, the anchor used was the free energy of Na^+ binding to dimethylacetamide (DMA, CH_3CONMe_2), 126.8 kJ/mol, which was derived from the TCID binding enthalpy measurement of Na^+DMA (156.9 kJ/mol at 298 K) performed by Klassen et al.,[9] who used a relatively tight TS assumption to extract their 0 K threshold values. In this same paper, the 0 K binding energy of Na^+G was measured as 151 ± 10 kJ/mol, 13 kJ/mol lower than the value measured in our laboratory using a loose PSL TS assumption. This suggests that the 0 K enthalpy value (ΔH_0) from Feng et al. might be increased by ~13 kJ/mol to 198 ± 16 kJ/mol, well within experimental error of our value. Other possible sources of error in this comparison include (a) that the correction from ΔG_{350} to ΔH_0 could be inaccurate because of the difficulties associated with the floppy motions of the dipeptide. (b) A complex sequence of studies was needed to yield the free energy for Na^+ binding to GG. The relative binding energies of DMA versus alanine, alanine versus leucine, leucine versus *N*-acetylleucine, *N*-acetylleucine versus glycylcysteine, and glycylcysteine versus GG were combined with the Na^+DMA anchor value to yield the final value for Na^+GG. Clearly, errors could accumulate in the five steps. (c) The effective ion temperature in the ion trap could be inaccurate.

Wesdemiotis and co-workers recently extended their kinetic method study of sodiated peptide systems from GG to GGG and GGGG using the Na^+ affinity of GG (203 ± 8 kJ/mol at 298 K) measured in the same laboratory as a reference.[15] The 298 K BDE value they obtained for Na^+GGG was 237 ± 9 kJ/mol (corresponding to 236 kJ/mol at 0 K), in excellent agreement with the 240 ± 20 kJ/mol TCID value measured in the present work (Table 3). The difference in BDE values for GG and GGG, which should be more precisely measured by both techniques, is 35 kJ/mol in the kinetic method study. This difference is in good agreement with our results, 31 kJ/mol, and with theoretical estimates that range from 36 to 47 kJ/mol (Table 3). It is noteworthy that the difference in BDEs for Na^+GG and Na^+GGG is over 110 kJ/mol if kinetic shifts are not accounted for, much larger than the values determined by the kinetic method or theory. This discrepancy underlines the importance of incorporating RRKM theory in modeling the experimental cross sections to obtain accurate thermochemical information. Wesdemiotis and co-workers[15] also reported a 298 K BDE of 261 ± 11 kJ/mol for Na^+ to GGGG, which corresponds to a 24 kJ/mol increase from GGG to GGGG. The trend of increasing BDE with increasing number of residues indicates that the coordination number for Na^+ increases with each residue but by a decreasing amount. This is consistent with a decreasing charge density on Na^+ as the number of ligand sites coordinating to Na^+ increases and with increased steric constraints.[69]

4.4. Comparison of Experimental and Theoretical BDEs. The theoretical BDEs for M^+L, where $M^+ = Na^+$ and K^+ and L = G, GG, and GGG, and Na^+G_2 complexes calculated at three levels of theory for all metal cations and those from the literature are compared to the present and literature experimental values in Table 3. Overall, these theoretical BDEs predict the same trends and agree reasonably well with the experimental values. We find that B3LYP or MP2(full) without counterpoise (cp) corrections give the largest values and are in the best agreement with the experimental values, whereas B3P86 and MP2(full) including cp are systematically low by small amounts. Mean absolute deviations (MADs) from the seven experimental BDEs are 5 ± 3, 6 ± 5, 12 ± 5, and 4 ± 3 kJ/mol for B3LYP, B3P86, and MP2(full) with and without cp levels of theory,

respectively. This gives confidence in these levels of theory to accurately describe these electrostatically bound complexes.

It can also be seen that the present theoretical values are comparable to those previously published for Na^+GG and Na^+GGG.[10,14,15,23,25] Differences are attributable to the somewhat different levels of theory used. The theoretical BDE for K^+GG from Wong et al.[25] is somewhat higher than the present calculations, even though the level of theory is comparable. (They used a slightly larger polarization basis set for single-point calculations and a somewhat smaller basis set for the geometry optimization, B3LYP/6-311+G(3df,2p)//B3LYP/6-31G(d).) The main difference appears to come from the different approach used to calculate the ZPEs for GG and K^+GG, which were taken from scaled HF/6-31G(d) calculations. In our work, all ZPEs are calculated at the same level of theory used for the final geometry optimization.

5. Conclusion

The kinetic energy dependences of the CID of M^+L, where $M^+ = Na^+$ and K^+ and L = GG and GGG, and Na^+G_2 were examined using a guided ion beam tandem mass spectrometer. The dominant dissociation pathway for M^+L and Na^+G_2 was the loss of an intact ligand from the complex. Small cross sections for the production of Na^+G were also found for TCID of Na^+GGG, a pathway explored in detail elsewhere.[71] Subsequent loss of the second ligand at high energy in Na^+G_2 also was seen. Absolute BDEs at 0 K for losing GG and GGG from M^+L and both G ligands from Na^+G_2 were obtained by analysis of the energy dependent cross sections. The final results are listed in Table 3 and resolve a discrepancy in the literature regarding the absolute BDE for Na^+GG. The experimental 0 K BDEs for M^+L, where L = G, GG, and GGG and $M^+ = Na^+$ and K^+, follow the order G < GG < GGG and can be related to the increasing polarizability of L (Figure 5). In addition, the BDEs follow the order $Na^+L > K^+L$ for all these systems. The BDE of the second G ligand to Na^+ is smaller than that of the first G ligand, but the sum of the Na^+-2G BDEs exceeds that for Na^+-GG, largely a consequence of the steric constraints associated with a single ligand versus two independent ligands.

Three different levels of ab initio calculations including ZPE and basis set superposition error corrections were performed for M^+L, where $M^+ = Li^+$, Na^+, and K^+ and L = GG and GGG, and Na^+G_2. All levels of theory predicted charge-solvated structures for M^+L and Na^+G_2. The metal cations prefer to bind in [CO,CO] bidentate or [N,CO,CO] tridentate configurations in M^+GG, a [CO,CO,CO] tridentate configuration in M^+GGG, and a [N,CO,N,CO] tetradentate configuration in Na^+G_2. The calculated BDEs for losing GG and GGG from Na^+L and K^+L agree very well with the present and some literature experimental values. Significantly, this good agreement relies on including kinetic shifts in the threshold measurements and on using a loose-phase space limit transition state for loss of the multidentate peptide. Good agreement also was found for the loss of both G ligands from Na^+G_2. Trends in the calculated BDEs agree with experiment in all facets. Overall, the present study confirms that accurate absolute thermodynamic information can be obtained from threshold CID studies of metal cationized small peptides.

Acknowledgment. This work was supported by the National Science Foundation under Grant CHE-0748790. A grant of computer time from the Center for High Performance Computing at the University of Utah is gratefully acknowledged. Bob Moision is thanked for help with MD simulations used in the present systems.

Supporting Information Available: Descriptions of geometries of low-lying conformers of GG, GGG, M^+GG, and M^+GGG where $M^+ = Li^+$, Na^+, and K^+ calculated at the B3LYP/6-311+G(d) level of theory. Two tables (S1 and S2) of relative energies of low-lying conformers of all species and one table (S3) of critical bond lengths and bond angles of neutral and metalated complexes. Four figures of optimized geometries of all low-lying conformers of GG (S1), GGG (S2), M^+GG (S3), and M^+GGG (S4) calculated at B3LYP/6-311+G(d) level. This information is available free of charge via the Internet at http://pubs.acs.org.

References and Notes

(1) Mathews, C. K.; van Holde, K. E. *Biochemistry*; The Benjamin Cummings Publishing Company: Redwood City, CA, 1990.
(2) Liu, Z.; Xu, Y.; Tang, P. *J. Am. Chem. Soc.* **2006**, *110*, 12789−12795.
(3) Feng, W. Y.; Gronert, S.; Lebrilla, C. B. *J. Phys. Chem. A* **2003**, *107*, 405−410.
(4) Cerda, B. A.; Wesdemiotis, C. *Analyst* **2000**, *125*, 657−660.
(5) Talley, J. M.; Cerda, B. A.; Ohanessian, G.; Wesdemiotis, C. *Chem.−Eur. J.* **2002**, *8*, 1377−1388.
(6) Moision, R. M.; Armentrout, P. B. *J. Phys. Chem. A* **2002**, *106*, 10350−10362.
(7) Kapota, C.; Lemaire, J.; Maitre, P.; Ohanessian, G. *J. Am. Chem. Soc.* **2004**, *126*, 1836−1842.
(8) Moision, R. M.; Armentrout, P. B. *Phys. Chem. Chem. Phys.* **2004**, *6*, 2588−2599.
(9) Klassen, J. S.; Anderson, S. G.; Blades, A. T.; Kebarle, P. *J. Phys. Chem.* **1996**, *100*, 14218−14227.
(10) Cerda, B. A.; Hoyau, S.; Ohanessian, G.; Wesdemiotis, C. *J. Am. Chem. Soc.* **1998**, *120*, 2437−2448.
(11) Cooks, R. G.; Wong, P. H. *Acc. Chem. Res.* **1998**, *31*, 379−386.
(12) Cooks, R. G.; Koskinen, J. T.; Thomas, P. D. *J. Mass Spectrom.* **1999**, *34*, 85−92.
(13) Feng, W. Y.; Gronert, S.; Lebrilla, C. B. *J. Am. Chem. Soc.* **1999**, *121*, 1365−1371.
(14) Kish, M. M.; Wesdemiotis, C.; Ohanessian, G. *J. Phys. Chem. B* **2004**, *108*, 3086−3091.
(15) Wang, P.; Wesdemiotis, C.; Kapota, C.; Ohanessian, G. *J. Am. Soc. Mass Spectrom.* **2007**, *18*, 541−552.
(16) Kish, M. M.; Ohanessian, G.; Wesdemiotis, C. *Int. J. Mass Spectrom.* **2003**, *227*, 509−524.
(17) Ryzhov, V.; Dunbar, R. C.; Cerda, B. A.; Wesdemiotis, C. *J. Am. Soc. Mass Spectrom.* **2000**, *11*, 1037−1046.
(18) Gapeev, A.; Dunbar, R. C. *J. Am. Chem. Soc.* **2001**, *123*, 8360−8365.
(19) Ruan, C.; Rodgers, M. T. *J. Am. Chem. Soc.* **2004**, *126*, 14600−14610.
(20) Shoeib, T.; Rodriquez, C. F.; Siu, K. W. M.; Hopkinson, A. C. *Phys. Chem. Chem. Phys.* **2001**, *3*, 853−861.
(21) Strittmatter, E. F.; Williams, E. R. *Int. J. Mass Spectrom.* **1999**, *185−187*, 935−948.
(22) Zhang, K.; Cassady, C. J.; Chung-Phillips, A. *J. Am. Chem. Soc.* **1994**, *116*, 11512−11521.
(23) Benzakour, M.; Mcharfi, M.; Cartier, A.; Daoudi, A. *J. Mol. Struct.* **2004**, *710*, 169−174.
(24) Wyttenbach, T.; Bushnell, J. E.; Bowers, M. T. *J. Am. Chem. Soc.* **1998**, *120*, 5098−5103.
(25) Wong, C. H. S.; Ma, N. L.; Tsang, C. W. *Chem.−Eur. J.* **2002**, *8*, 4909−4918.
(26) Ervin, K. M.; Armentrout, P. B. *J. Chem. Phys.* **1985**, *83*, 166−189.
(27) Muntean, F.; Armentrout, P. B. *J. Chem. Phys.* **2001**, *115*, 1213−1228.
(28) Gerlich, D. *Adv. Chem. Phys.* **1992**, *82*, 1−176.
(29) Daly, N. R. *Rev. Sci. Instrum.* **1960**, *31*, 264−267.
(30) Hales, D. A.; Lian, L.; Armentrout, P. B. *Int. J. Mass Spectrom. Ion Processes* **1990**, *102*, 269−301.
(31) Moision, R. M.; Armentrout, P. B. *J. Am. Soc. Mass Spectrom.* **2007**, *18*, 1124−1134.
(32) Shaffer, S. A.; Prior, D. C.; Anderson, G. A.; Udseth, H. R.; Smith, R. D. *Anal. Chem.* **1998**, *70*, 4111−4119.
(33) Shaffer, S. A.; Tolmachev, A.; Prior, D. C.; Anderson, G. A.; Udseth, H. R.; Smith, R. D. *Anal. Chem.* **1999**, *71*, 2957−2964.
(34) Schultz, R. H.; Crellin, K. C.; Armentrout, P. B. *J. Am. Chem. Soc.* **1991**, *113*, 8590−8601.
(35) Fisher, E. R.; Armentrout, P. B. *J. Chem. Phys.* **1991**, *94*, 1150−1157.

(36) Fisher, E. R.; Kickel, B. L.; Armentrout, P. B. *J. Chem. Phys.* **1992**, *97*, 4859−4870.
(37) Rodgers, M. T.; Armentrout, P. B. *J. Phys. Chem. A* **1997**, *101*, 1238−1249.
(38) Rodgers, M. T.; Armentrout, P. B. *Int. J. Mass Spectrom.* **1999**, *185*−*187*, 359−380.
(39) Rodgers, M. T.; Armentrout, P. B. *J. Phys. Chem. A* **1999**, *103*, 4955−4963.
(40) Moision, R. M.; Armentrout, P. B. *J. Phys. Chem. A* **2006**, *110*, 3933−3946.
(41) Beyer, T. S.; Swinehart, D. F. *Commun. Assoc. Comput. Machinery* **1973**, *16*, 379.
(42) Rodgers, M. T.; Ervin, K. M.; Armentrout, P. B. *J. Chem. Phys.* **1997**, *106*, 4499−4508.
(43) Rodgers, M. T.; Armentrout, P. B. *J. Chem. Phys.* **1998**, *109*, 1787−1800.
(44) Gilbert, R. G.; Smith, S. C. *Theory of Unimolecular and Recombination Reactions*; Blackwell Scientific: London, 1990.
(45) Truhlar, D. G.; Garrett, B. C.; Klippenstein, S. J. *J. Phys. Chem.* **1996**, *100*, 12771−12800.
(46) Holbrook, K. A.; Pilling, M. J.; Robertson, S. H. *Unimolecular Reactions*, 2nd ed.; Wiley: New York, 1996.
(47) Meyer, F.; Khan, F. A.; Armentrout, P. B. *J. Am. Chem. Soc.* **1995**, *117*, 9740−9748.
(48) Koizumi, H.; Armentrout, P. B. *J. Am. Soc. Mass Spectrom.* **2001**, *12*, 480−489.
(49) Ye, S. J.; Moision, R. M.; Armentrout, P. B. *Int. J. Mass Spectrom.* **2006**, *253*, 288−304.
(50) More, M. B.; Ray, D.; Armentrout, P. B. *J. Phys. Chem. A* **1997**, *101*, 831−839.
(51) More, M. B.; Ray, D.; Armentrout, P. B. *J. Phys. Chem. A* **1997**, *101*, 4254−4262.
(52) More, M. B.; Ray, D.; Armentrout, P. B. *J. Phys. Chem. A* **1997**, *101*, 7007−7017.
(53) Waage, E. V.; Rabinovitch, B. S. *Chem. Rev.* **1970**, *70*, 377−387.
(54) Armentrout, P. B.; Simons, J. *J. Am. Chem. Soc.* **1992**, *114*, 8627−8633.
(55) Pearlman, D. A.; Case, D. A.; Caldwell, J. W.; Ross, W. R.; Cheatham, T. E.; DeBolt, S.; Ferguson, D.; Seibel, G.; Kollman, P. *Comput. Phys. Commun.* **1995**, *91*, 1−41.
(56) Bylaska, E. J.; de Jong, W. A.; Kowalski, K.; Straatsma, T. P.; Valiev, M.; Wang, D.; Aprà, E.; Windus, T. L.; Hirata, S.; Hackler, M. T.; Zhao, Y.; Fan, P.-D.; Harrison, R. J.; Dupuis, M.; Smith, D. M. A.; Nieplocha, J.; Tipparaju, V.; Krishnan, M.; Auer, A. A.; Nooijen, M.; Brown, E.; Cisneros, G.; Fann, G. I.; Früchtl, H.; Garza, J.; Hirao, K.; Kendall, R.; Nichols, J. A.; Tsemekhman, K.; Wolinski, K.; Anchell, J.; Bernholdt, D.; Borowski, P.; Clark, T.; Clerc, D.; Dachsel, H.; Deegan, M.; Dyall, K.; Elwood, D.; Glendening, E.; Gutowski, M.; Hess, A.; Jaffe, J.; Johnson, B.; Ju, J.; Kobayashi, R.; Kutteh, R.; Lin, Z.; Littlefield, R.; Long, X.; Meng, B.; Nakajima, T.; Niu, S.; Pollack, L.; Rosing, M.; Sandrone, G.; Stave, M.; Taylor, H.; Thomas, G.; Lenthe, J. V.; Wong, A.; Zhang, Z. *NWChem, A Computational Chemistry Package for Parallel Computers*, Version 4.5; Pacific Northwest National Laboratory: Richland, WA, 2003.
(57) Roothaan, C. C. *Rev. Mod. Phys.* **1951**, *23*, 69−89.
(58) Binkley, J. S.; Pople, J. A.; Hehre, W. J. *J. Am. Chem. Soc.* **1980**, *102*, 939−947.
(59) Frisch, M. J.; Trucks, G. W.; Schlegel, H. B.; Scuseria, G. E.; Robb, M. A.; Cheeseman, J. R.; Montgomery, J. A., Jr.; Vreven, T.; Kudin, K. N.; Burant, J. C.; Millam, J. M.; Iyengar, S. S.; Tomasi, J.; Barone, V.; Mennucci, B.; Cossi, M.; Scalmani, G.; Rega, N.; Petersson, G. A.; Nakatsuji, H.; Hada, M.; Ehara, M.; Toyota, K.; Fukuda, R.; Hasegawa, J.; Ishida, M.; Nakajima, T.; Honda, Y.; Kitao, O.; Nakai, H.; Klene, M.; Li, X.; Knox, J. E.; Hratchian, H. P.; Cross, J. B.; Adamo, C.; Jaramillo, J.; Gomperts, R.; Stratmann, R. E.; Yazyev, O.; Austin, A. J.; Cammi, R.; Pomelli, C.; Ochterski, J. W.; Ayala, P. Y.; Morokuma, K.; Voth, G. A.; Salvador, P.; Dannenberg, J. J.; Zakrzewski, V. G.; Dapprich, S.; Daniels, A. D.; Strain, M. C.; Farkas, O.; Malick, D. K.; Rabuck, A. D.; Raghavachari, K.; Foresman, J. B.; Ortiz, J. V.; Cui, Q.; Baboul, A. G.; Clifford, S.; Cioslowski, J.; Stefanov, B. B.; Liu, G.; Liashenko, A.; Piskorz, P.; Komaromi, I.; Martin, R. L.; Fox, D. J.; Keith, T.; Al-Laham, M. A.; Peng, C. Y.; Nanayakkara, A.; Challacombe, M.; Gill, P. M. W.; Johnson, B.; Chen, W.; Wong, M. W.; Gonzalez, C.; Pople, J. A. *Gaussian 03*, Revision B.02; Gaussian, Inc.: Pittsburgh, PA, 2003.
(60) Becke, A. D. *J. Chem. Phys.* **1993**, *98*, 5648−5652.
(61) Lee, C.; Yang, W.; Parr, R. G. *Phys. Rev. B: Condens. Matter Mater. Phys.* **1988**, *37*, 785−789.
(62) Petersson, G. A.; Tensfeldt, T.; Montgomery, J. A. *J. Chem. Phys.* **1991**, *94*, 6091−6101.
(63) McLean, A. D.; Chandler, G. S. *J. Chem. Phys.* **1980**, *72*, 5639−5648.
(64) Krishnan, R.; Binkley, J. S.; Seeger, R.; Pople, J. A. *J. Chem. Phys.* **1980**, *72*, 650−654.
(65) Foresman, J. B.; Frisch, A. E. *Exploring Chemistry with Electronic Structure Methods*, 2nd ed.; Gaussian, Inc.: Pittsburgh, PA, 1996.
(66) van Duijneveldt, F. B.; van Duijneveldt de Rijdt, J. G. C. M.; van Lenthe, J. H. *Chem. Rev.* **1994**, *94*, 1873−1885.
(67) Ye, S. J.; Moision, R. M.; Armentrout, P. B. *Int. J. Mass Spectrom.* **2005**, *240*, 233−248.
(68) Armentrout, P. B.; Rodgers, M. T. *J. Phys. Chem. A* **2000**, *104*, 2238−2247.
(69) Rodgers, M. T.; Armentrout, P. B. *Acc. Chem. Res.* **2004**, *37*, 989−998.
(70) Rodgers, M. T.; Armentrout, P. B. *Mass Spectrom. Rev.* **2000**, *19*, 215−247.
(71) Ye, S.; Armentrout, P. B., work in progress.
(72) Armentrout, P. B. *J. Chem. Phys.* **2007**, *126*, 234302−1−9.
(73) Rodriguez-Santiago, L.; Sodupe, M.; Tortajada, J. *J. Phys. Chem. A* **2001**, *105*, 5340−5347.
(74) Pulkkinen, S.; Noguera, M.; Rodriguez-Santiago, L.; Sodupe, M.; Bertran, J. *Chem.—Eur. J.* **2000**, *6*, 4393−4399.
(75) Moision, R. M.; Armentrout, P. B., work in progress.
(76) Lee, S.; Wyttenbach, T.; Bowers, M. T. *Int. J. Mass Spectrom.* **1997**, *167*−*168*, 605−614.
(77) Wilson, R. G.; Brewer, G. R. *Ion Beams with Applications to Ion Implantation*; Wiley: New York, 1973.
(78) Smith, S. M.; Markevitch, A. N.; Romanov, D. A.; Li, X.; Levis, R. J.; Schlegel, H. B. *J. Phys. Chem. A* **2004**, *108*, 11063−11072.
(79) Ye, S. J.; Clark, A. A.; Armentrout, P. B. *J. Phys. Chem. B* **2008**, submitted.
(80) Dalleska, N. F.; Tjelta, B. L.; Armentrout, P. B. *J. Phys. Chem.* **1994**, *98*, 4191−4195.
(81) Bojesen, G.; Breindahl, T.; Andersen, U. N. *Org. Mass Spectrom.* **1993**, *28*, 1448−1452.
(82) Hoyau, S.; Ohanessian, G. *Chem.—Eur. J.* **1998**, *4*, 1561−1569.